

**LORENTZ-SHAPED COMET DUST TRAIL CROSS SECTION
FROM NEW HYBRID VISUAL AND VIDEO METEOR
COUNTING TECHNIQUE – IMPLICATIONS FOR FUTURE
LEONID STORM ENCOUNTERS**

**PETER JENNISKENS, CHRIS CRAWFORD¹, STEVEN J. BUTOW,
AND DAVID NUGENT**

*SETI Institute, NASA/Ames Research Center, Mail Stop 239-4, Moffett Field, CA
94035, USA; ¹) 2349 Sterling Creek Road, Jacksonville, OR 97530, USA
E-mail: pjenniskens@mail.arc.nasa.gov*

MIKE KOOP, DAVID HOLMAN, AND JANE HOUSTON
California Meteor Society, 1037 Wunderlich Drive, San Jose, CA 95129-3159, USA

KLAAS JOBSE
Dutch Meteor Society, Lederkarper 4, 2318 NB Leiden, The Netherlands

GARY KRONK
*American Meteor Society, North American Meteor Network, 1117 Troy-O'fallon Road,
Troy, Il 62294, USA*

and

KELLY BEATTY
Sky & Telescope, 49 Bay State Road, Cambridge, MA 02138-1200, USA

(Received 4 June 2000; Accepted 18 August 2000)

Abstract. A new hybrid technique of visual and video meteor observations was developed to provide high precision near real-time flux measurements for satellite operators from airborne platforms. A total of 33,000 Leonids, recorded on video during the 1999 Leonid storm, were watched by a team of visual observers using a video head display and an automatic counting tool. The counts reveal that the activity profile of the Leonid storm is a Lorentz profile. By assuming a radial profile for the dust trail that is also a Lorentzian, we make predictions for future encounters. If that assumption is correct, we passed 0.0003 AU deeper into the 1899 traillet than expected during the storm of 1999 and future encounters with the 1866 traillet will be less intense than predicted elsewhere.

Keywords: Comet, comet: 55P/Tempel-Tuttle, dust trail, flux, Leonids 1999, Lorentz profile, meteor, meteor storm, predictions, satellite impact hazard, observing techniques

1. Introduction

The requirement for near-real time flux measurements from aircraft (Jenniskens and Butow, 1999) has led to the development of a hybrid technique of visual and video meteor observations. The method has a team of visual meteor observers view the video output of intensified cameras using video head displays (Figure 1). The cameras make it possible to conveniently observe part of the sky with a well defined field of view. The method proves particularly successful for airborne applications. The cameras are mounted behind optical windows in the aircraft and pointed at relatively low altitude, which achieves 3-4 times higher counts than from the ground (Jenniskens, 1999). We further boost the meteor count by visually inspecting the tapes rather than using automatic meteor detection software programs. The results enable a precise analysis of the 1999 Leonid storm rate profile. Of particular interest are the shape of the profile and possible deviations from a smooth mean behavior, which provide information about the ejection mechanism and shower dynamics in the planetary environment.

2. The Method

During the 1999 Leonid MAC mission, a team of eight visual observers first demonstrated this new approach on-board the "*Advanced Ranging and Instrumentation Aircraft (ARIA)*", operated by the USAF/452nd Flight Test Squadron. Details of the flight path and observing conditions are given in Jenniskens *et al.* (2000).

A counting tool was developed that records the detection of Leonid shower or sporadic meteors with the click of a mouse button. The tool has six entrance ports, which recorded the counts from one of six different intensified cameras. The four cameras considered here had a field of view of $39^\circ \times 29^\circ$ and were mounted at an elevation of about 22° behind BK7 optical glass windows.

Each observer was assigned a mouse bearing a unique machine-readable identification number; each camera had its own designated computer port. The mice were chosen for their ergonomic design and their light-response buttons. The observer began each observing session by plugging the mouse into the computer port corresponding to the camera being used by the observer; the mouse was unplugged at the end

of each viewing session. This permitted the computer to identify the starting and ending times of each viewing session, and determine which observer was watching from what camera at all times. Rotating the observer/camera pairings enabled calculation of individual observer and camera coefficients of perception from systematic differences in the counts.



Figure 1. Observer Jane Houston with video head display.

During the 1999 Leonid meteor storm, ARIA flew from the UK to Israel, from Israel to the Azores, and from the Azores to Florida on three consecutive nights. The peak of the storm occurred while enroute from Greece to Italy. Near-real time flux measurements were automatically transferred to a communication station on-board the aircraft, where the counts were sent to NASA/Ames Research Center by e-mail, telephone or direct internet access using INMARSAT satellite telephone lines. From NASA/ARC, the counts were further distributed to operation centers, such as the NASA and USAF sponsored LEOC at Marshall Space Flight Center and ESA's orbital debris center at ESOC, Darmstadt.

Shortly after the mission, several observers gathered at NASA/Ames Research Center to view, in the same manner, the video tapes that were recorded by four similar intensified cameras on-board the twin "*Flying Infrared Signature Technology Aircraft (FISTA)*". FISTA was about 150 km north from ARIA and the bulk of meteors are independent records.

3. Results

3.1. THE STORM PEAK

A total of 33,000 video Leonids were recorded in this manner, which account for about 3/4 of all Leonids on video. This compares with 277,172 Leonids that were observed by 434 visual observers worldwide and gathered by the International Meteor Organisation (Arlt *et al.* 1999). Both data sets will be discussed together. The video data will be shown by black points, the previously published visual data by open squares. Although the number of video meteors is 8 times less than the visual record, the measurements are performed under much better controlled conditions, from which a more precise result can be expected.

Figure 2 shows the peak of the storm. No smoothing was applied. Individual points are 1-minute intervals. Each interval is an independent measurement. The video data are very smooth. The curve is featureless. A small depression at the peak can not be trusted because it is not present in the ARIA and FISTA data in the same way. We suspect that muscle fatigue in the button-pressing fingers started to become a problem at about that time. In hindsight, it appears that the technique works well for rates between ZHR = 5 and 5,000, but the technique will need modifications to conveniently cope with higher rates.

In this paper, our video rates are scaled to the visual Zenith Hourly Rates calculated by Arlt *et al.* (1999). The rates of Arlt *et al.* represent independent intervals of 2.8 minutes. We are not concerned with the absolute values, but with the shape of the curve. Hence, all data are plotted on a logarithmic scale, so that any scaling is a mere shift in the graph.

It is a compliment to the ground-based amateur visual observers and the airborne video observers to see how well both datasets agree! The time of the peak is confirmed at solar longitude $\lambda_0 = 235.285 \pm 0.001^\circ$, or $t = 02:00.8 \pm 1.5$ min. UT (with $\Delta t = -0.5$ min topocentric correction following McNaught and Asher, 1999a). Also, the slopes of the activity profile are much the same. The visual data show more scatter around the mean, despite the higher number of meteors in each count. The profile is very smooth. We do not confirm the "additional clear enhancements" (Arlt *et al.*, 1999), which were thought to be features in shower models.

These are probably the result of imperfect corrections for observer perception, observing conditions or other factors that affect visual observations. For the same reason, such features in the profiles from individual locations can not be trusted. In the remainder of this paper, we will concentrate on the gross features of the curves that are confirmed by both video and visual results.

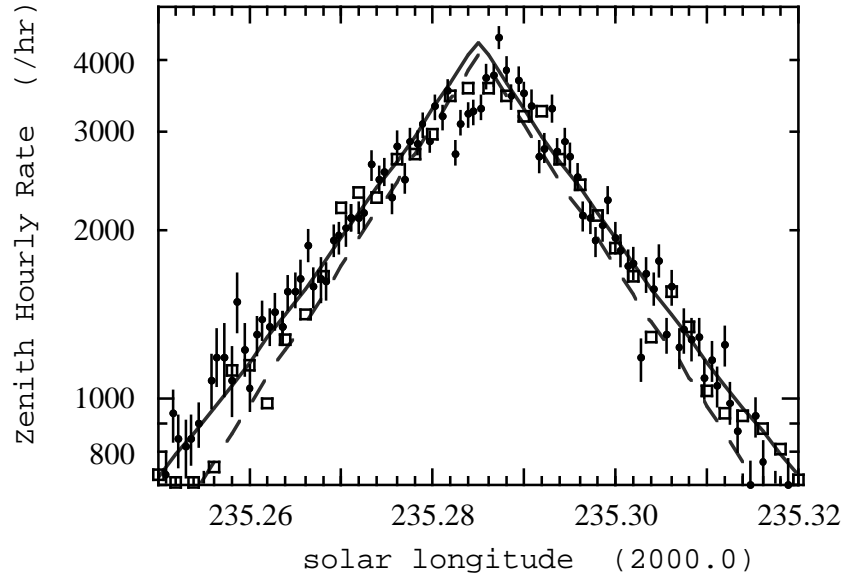


Figure 2. The peak of the 1999 Leonid storm. Solid points are our 1-minute counts (no smoothing applied). Open squares are data from Arlt *et al.* (1999). The dashed line shows the storm component (main peak), while the solid line is the best fit of all components together.

When plotted on a logarithmic scale, as in Figure 2, it is clear that the slopes of the storm peak are linear and well represented by an exponential equation like (Jenniskens, 1995):

$$ZHR = ZHR_{\max} 10^{-B |\lambda_o - \lambda_o^{\max}|} \tag{1}$$

From a least squares fit, we find $B = 24 \pm 2$ per degree solar longitude for ZHR larger than 700. A slightly larger $B = 25 \pm 1$ value (and $ZHR_{\max} = 4,100$ per hour) results when a composite of such curves is fitted to the

profile that also accounts for other more shallow features. Note that this value is slightly less than the $B = 30 \pm 3$ derived from the 1866, 1867, 1966 and 1969 Leonid storm profiles (Jenniskens, 1995), when Earth crossed deeper into the respective trail.

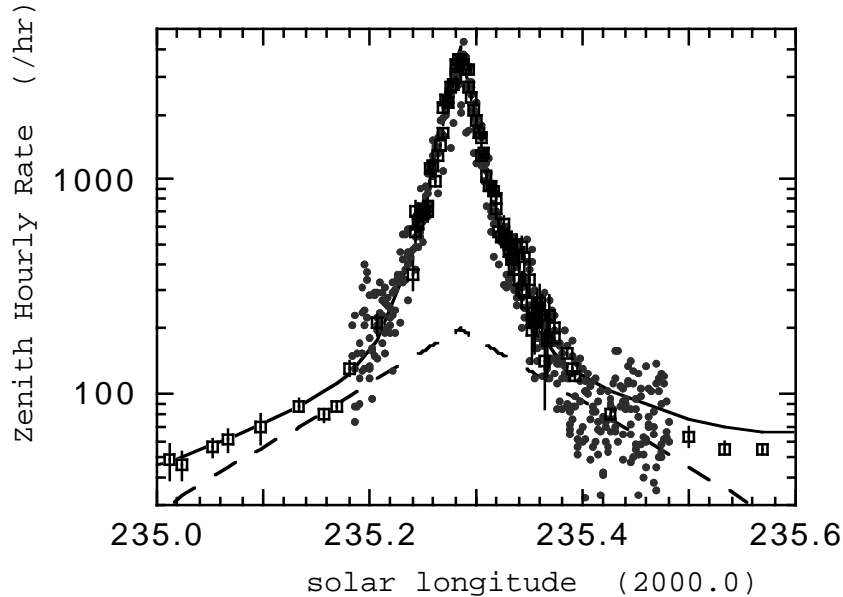


Figure 3. Wings of the profile, with background to the main peak indicated by a dashed line. Symbols as in Figure 2.

Above solar longitude $\lambda_0 = 235.38$ (and below 235.20), rates level off significantly in both video and visual data (Figure 3). A similar background structure to the main peak was observed in the 1866 and 1867 profiles (Jenniskens, 1995). The slopes are near linear again on a logarithmic scale, with $B = 2.5 \pm 0.2$. Combined with the annual Leonid background, we have $B = 3.0 \pm 0.3$ for this component, slightly less than found before ($B = 4-6$), but typically from a smaller part of the activity profile. This structure appears to be centered within 0.01° from the center of the storm peak. When we assume the same peak time, we have a peak rate of $ZHR_{\max} = 200 \pm 10$.

From the visual data (Arlt *et al.*, 1999), we conclude that the magnitude distribution index does not seem to change over the peak. This implies that the magnitude distribution index of the background component and main peak are the same (as we surmised earlier from the

1866 and 1966 profiles - Jenniskens, 1995). And that suggests strongly that both components are caused by the same physical processes, with no intrinsic merit to make a distinction between the two components. We expect to be able to verify from the video record that the two components can not be discriminated on ground of the magnitude distribution index, but will take this as a task for a future paper.

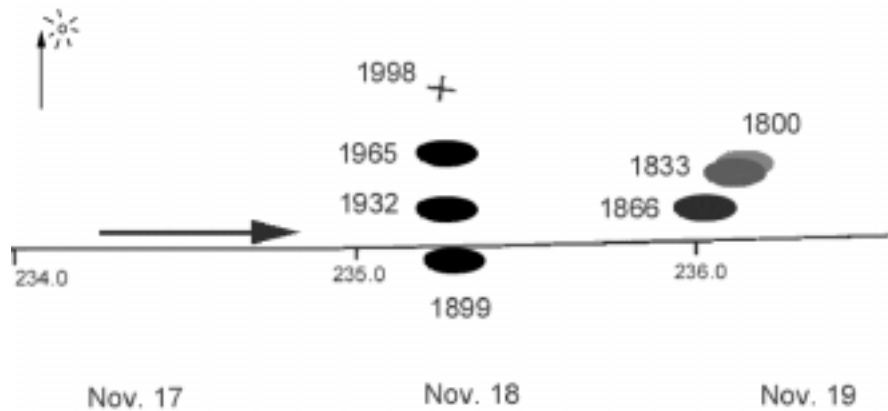


Figure 4. The Earth's path by debris trails ejected at various epochs during the return of 1999. Courtesy: David Asher, Armaugh Observatory.

3.2. THE 1866 TRAILET

This material is thought to have been ejected in 1899 (Kondratieva and Reznikov, 1985; McNaught and Asher, 1999b; Lyytinen, 1999). In Asher's diagrams of the path of Earth through the meteor shower, reproduced in Figure 4, the Earth approaches dust trails from 1866, 1833 and 1800 shortly after passing the 1899 and 1932 trails. Earlier during the 1998 return, we observed a peak in activity when Earth passed rather far from the calculated center of the 1899 debris trail (Jenniskens, 1999). Hence, we anticipated a second peak of activity just after solar longitude 236.0. Based on observations from Hawaii, Japan and China, Arlt *et al.* (1999) show this second maximum peak at solar longitude 235.87 ± 0.04 . Leonid MAC observations in the night after the main peak show enhanced rates that appear to trace the declining branch of this component, showing a relatively fast decline (Figure 5). A curve with $B = 1.6$ would best fit the descending branch. However, a symmetric curve

with this B value would raise the saddle between the two peaks and doesn't make a good fit to the ascending part.

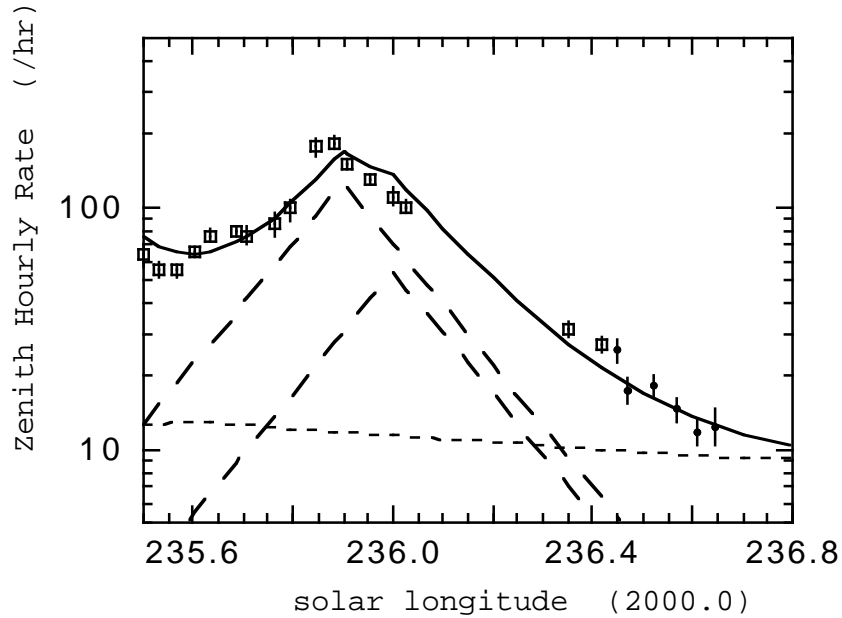


Figure 5. The second peak in the activity curve related to the 1866, 1833 and 1800 trails. Symbols as in Figure 2. The horizontal dashed line with narrow spacing shows the annual Leonid shower activity. Two other dashed lines show the contributions from the 1866 (left) and 1833/1800 (right) trails. The solid line is the combination of all components.

In light of Figure 4, we interpret this peak as a composite of the result of several traillets. Hence, we fitted two sets of curves with $B = 3.0$ to the data, peaking at solar longitude of 235.90 ($ZHR_{\max} = 125$) and 236.00 ($ZHR_{\max} = 50$). That separation was taken to reflect the calculations by McNaught and Asher (1999b). However, the second peak occurred 0.14 degrees earlier than predicted, if the nearest point in Earth's orbit to the traillet center at the point of ecliptic plane crossing is considered. It follows that the current model does not precisely describe the position of the trails, at least not for later revolutions or trails at some distance from Earth's path.

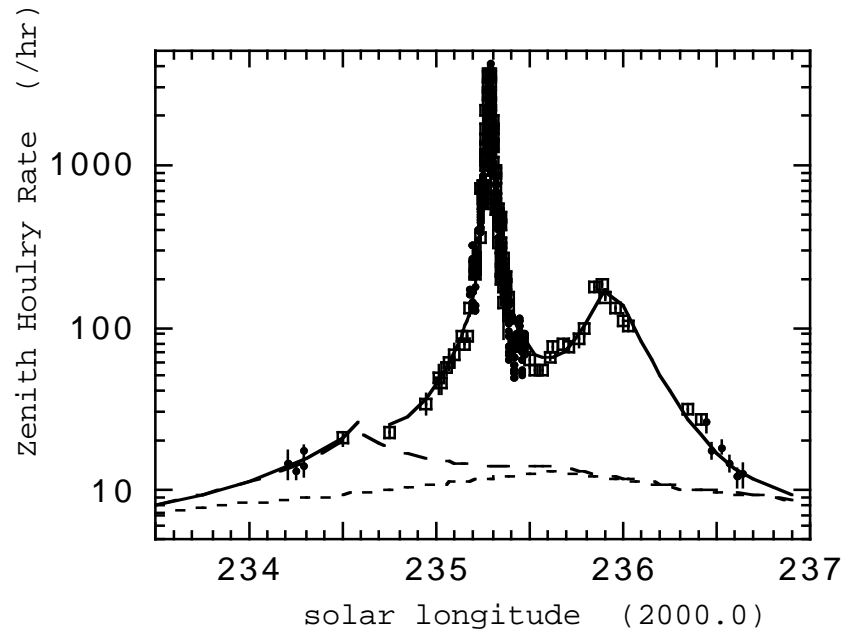


Figure 6. Possible presence of the Leonid Filament component (solid line). Symbols as in Figures 2 and 5.

3.3. THE LEONID FILAMENT?

In prior years, another dust component called the Leonid Filament was responsible for fireball showers in all years from 1994 until 1998 (Jenniskens, 1996). Its characteristic feature is the width, with $B = 1.1 \pm 0.1$ in all years, and its low magnitude distribution index. Jenniskens and Betlem (2000) predicted a return of this component at a lower level than in 1998, assuming that the Filament was the accumulation of many years of dust ejecta. Asher (1999), on the other hand, predicted no activity at all if the Filament was due to ejecta of the return of 1333 only.

The 1999 profile does not show a clear broad component that is readily defined as the Leonid Filament. This appears to confirm Asher's prediction. However, Leonid MAC observations in the night prior to the peak night (at solar longitude 234.5) show a significant enhancement of rates above expected levels that may in fact be caused by the Filament. The expected level being a mere extrapolation of the contribution from the annual Leonid shower, the main and background storm peak, and the second 1866/1833 component (Figure 6). This is consistent with few

data shown in Arlt *et al.* (1999), which together trace a broader structure some time before the onset of the storm. Assuming that this is a profile with $B = 1.1$, that is caused by the Filament, then it has to peak at solar longitude 234.6 ± 0.2 with a peak rate of $ZHR = 13 \pm 2$. The profile can not extend much more to higher solar longitude, because that would create a hump near the peak of the profile. In that case, the component is weaker than the $ZHR \sim 120$ expected (Jenniskens and Betlem, 2000) and peaked earlier than the expected ~ 235.1 , but not far from the time of the 1998 peak.

Typically, this component has a significantly lower magnitude distribution index than the other shower components. We measured $r \sim 2.1$ on Nov. 16/17, which is the value expected. However, this value was based on meteor magnitudes called out by visual observers and represents only a very small fraction of observed meteors. A more complete magnitude analysis of the data can reveal if the proposed shower components are correct.

4. Discussion

In the past, shower profiles have been described in terms of Gaussian and exponential shapes (Jenniskens, 1995; Brown *et al.*, 1997). Now, we find that the Lorentz profile, known from damped oscillators, has a shape very similar to the peak and background combined:

$$ZHR = ZHR_{\max} \frac{(W / 2)^2}{(\lambda_o - \lambda_o^{\max})^2 + (W / 2)^2} \quad (2)$$

W is the classical width of the profile at half the peak intensity (in degrees). Indeed, the main peak above $ZHR = 300$ is best fitted with a Lorentz profile of width $W = 0.036 \pm 0.002^\circ$ and $ZHR_{\max} = 3300 \pm 100$, the line shown in Figure 7. The width is the only parameter that describes the shape of the curve. Indeed, the tail of the curve falls right on when the peak is fitted even if we ignore the background component.

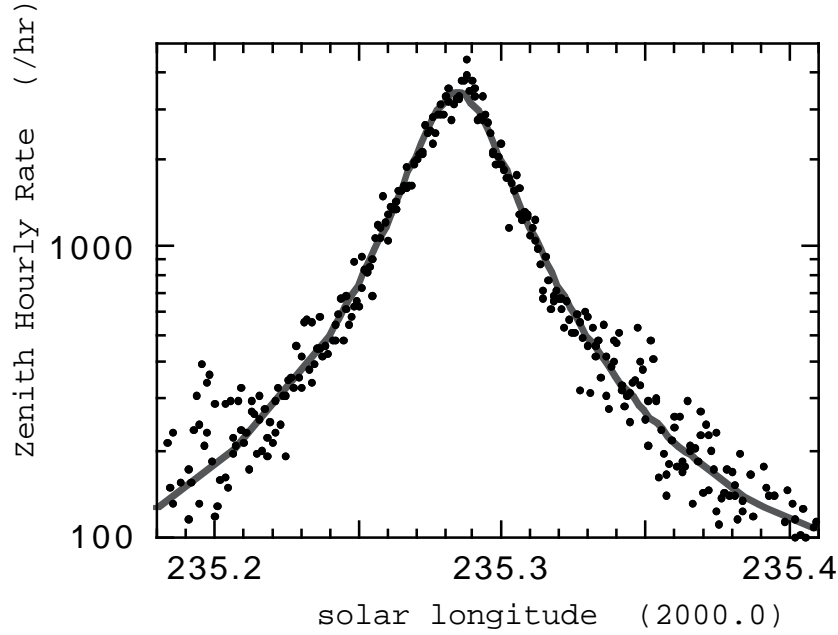


Figure 7. Fit of a Lorentz profile to the meteor storm profile. In order to bring out the small dispersion, error bars are not shown.

We find that data from past meteor storms show a similar good fit (Table I), which implies that each dust traillet itself has a Lorentzian cross section. This condition is necessary to account for the fact that we passed the dust traillets at different distances from the center in 1999, 1966 and 1866. If the dust distribution in a traillet (index "t") follows a Lorentz function as a function of r = distance from traillet center, then:

$$\text{ZHR}(r) = \text{ZHR}_{\text{max}}^t \frac{(W_t / 2)^2}{r^2 + (W_t / 2)^2} \quad (3)$$

In that case, the cross section is also Lorentzian if we pass the center of the traillet along the Earth's orbit in a direction $X = \lambda_o$ (now in AU, with roughly $2 \pi \text{ AU} = 360$ degrees neglecting curvature of the Earth's path) at a distance $Y = Y_o$ (measured in a direction perpendicular to Earth's orbit). Because, by substituting $r^2 = Y_o^2 + (X - X_o)^2$:

$$\text{ZHR}(X) = \text{ZHR}_{\max} \frac{Y_0^2 + (W_t/2)^2}{(X - X_0)^2 + Y_0^2 + (W_t/2)^2} \quad (4)$$

which has a similar form as Equation 3. In that case, the width of the dust traillet equals:

$$(W_t/2)^2 = (W/2)^2 - Y_0^2 \quad (5)$$

and the peak rate in the traillet is:

$$\text{ZHR}_{\max}^t = \text{ZHR}_{\max} \frac{(W/2)^2}{(W/2)^2 - Y_0^2} \quad (6)$$

The peak of a Lorentzian is in fact well represented by the exponential curves used before (Equation 1). The new representation only adds a tail to the distribution, which is assumed to be a natural consequence of the dispersion mechanism.

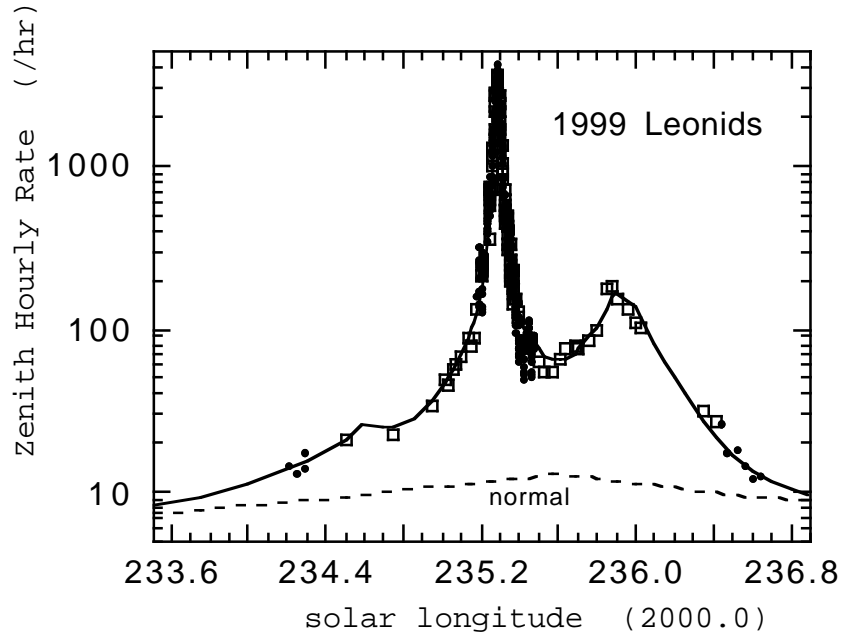


Figure 8. A fit of three Lorentzian curves to the activity profile, which describe the 1899-1932 trails (storm), the 1866-1800 trails (2nd peak) and the Filament. Symbols as in Figures 2 and 5.

It is not clear, at present, what physical mechanism is responsible for this tail in the distribution. Lorentzian distributions are characteristic for damped oscillators, and perhaps a natural consequence of the orbital evolution in the three body system meteoroid-Sun-Jupiter.

Given the good representation in the case of the 1999 Leonid storm, we applied the Lorentzian fit to other shower components (Table I). We find that this year's shower profile is well represented with three Lorentz curves representing storm, 1866 peak, and Filament (Figure 8).

TABLE I

Year	From	$\Delta C-E$ *	M_o **	W/2	ZHR_{max}	λ_o^{max}
		(AU)	($^{\circ}$)	(AU)	(hr^{-1})	($^{\circ}$)
<i>observed:</i>						
1999	1899	-0.0007	18.4	0.00031 \pm 0.00002	3,300 \pm 100	235.285
1998	1899	(+0.0044)#	16.6	0.00087 \pm 0.00008	70 \pm 20	(235.28)#
1966	1899	-0.0001	16.6	0.00024 \pm 0.00005	15,000 \pm 3000	235.166
1965	1899	+0.0017	5.8	0.0024 \pm 0.0007	100 \pm 50	235.40
1969	1932	+0.0000	49.1	0.00026 \pm 0.00005	200 \pm 50	235.265
1999	1866	+0.0016	19.0	0.0027 \pm 0.0003	130 \pm 15	235.95
1998	1866	+0.0040	16.6	0.003 \pm 0.002	10 \pm 10	236.0
1866	1733	-0.0004	9.1	0.00024 \pm 0.00007	14,000 \pm 2000	233.323
1867	1833	-0.0002	19.9	0.00024 \pm 0.00012	5,000 \pm 1000	233.411
<i>predicted:</i>						
2000	1866	+0.0008	29.5	(0.0011)	(70)	236.28 *
2000	1932	-0.0012	29.5	(0.0009)	(207)	235.29 *
2001	1866	+0.0002	40.3	(0.00053)	(72)	236.46 *
2002	1866	+0.0000	51.1	(0.00035)	(38)	236.86 *
2002	1966	+0.0018	51.1	(0.0021)	(4)	235.27 *

*) Minimum distance between Earth and Comet orbit, from McNaught & Asher (1999b)

***) Mean anomaly of trail particles

#) Large uncertainty because of perturbation by Earth in earlier encounter

From older data, we note that especially the 1966 profile as calculated by Brown *et al.* (1997) is a perfect Lorentzian, and not a Gaussian as proposed there. The "storm" peak of 1998 (Jenniskens, 1999) is an exception. That profile was clearly assymmetric, which differs from a Lorentzian profile. A sum of two profiles could fit that curve, but it is not easy to assign the components to the debris of a particular return. Perhaps, this debris was disturbed by prior close encounter with the planets, as proposed in McNaught and Asher (1999b). We do recognize an enhancement that can be associated with the passage of the 1866/1833/1800 traillets, in order to account for relatively high rates in the night after the maximum (Arlt and Brown, 1998; Jenniskens, 1999).

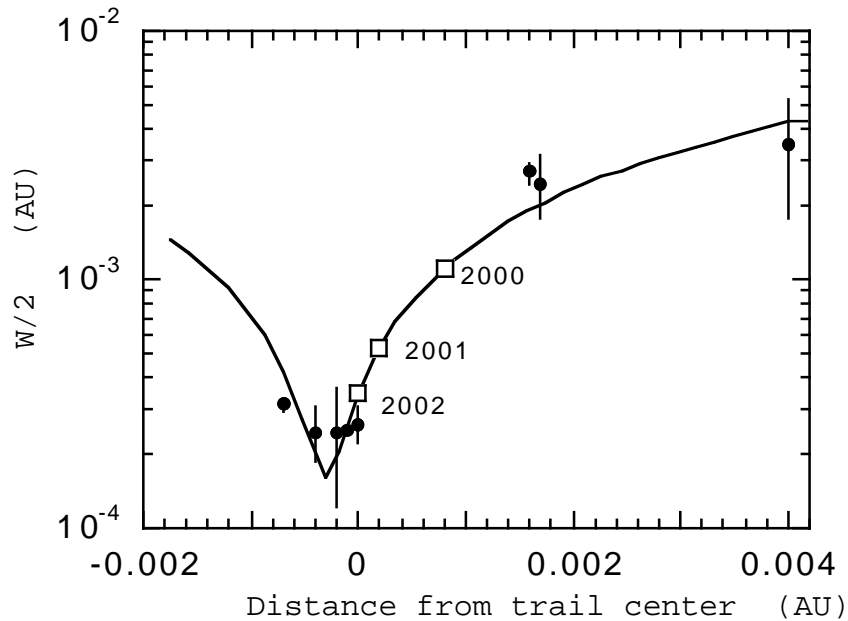


Figure 9. The width of the profile as a function of distance from the center of the traillet. The solid points are observations (Table I), the open squares are predicted values based on the fitted Lorentz curve (solid line).

The width of the profile is expected to gradually increase if the Earth passes further away from the center of the traillet. Near the center is a core with a steep slope, which has a more shallow tail further out. The core is typical for the 1866, 1867, 1966, 1969 and 1999 profiles, while

the profiles of 1998, 1965 and the second peak of 1999 are cases of further out. If we plot the width versus the distance to the traillet center (Y_0), as calculated by McNaught and Asher (1999b), then we find that Equation 5 (solid line in Figure 9) indeed does fit the result, allowing for at least ± 0.0001 AU uncertainty in the calculated traillet positions. The intrinsic width of the dust traillet is calculated at $W_t = 0.00032 \pm 0.00008$ AU.

However, the fit is good only if the calculated traillet pattern (together making up the comet dust trail) is shifted outward by about $+0.0003$ AU. The curve in Figure 9 should center on zero. We conclude that the Earth crossed about 0.0003 AU deeper into the debris trail ejected in 1899 than predicted. Unfortunately, that means that the Earth will not cross quite as deep into the 1866 epoch traillet in 2001 and 2002.

On top of that are two more factors that influence the peak rate in future years: 1) the rate of decrease of dust density away from the comet for a pristine traillet of 1 revolution, and 2) the decay of dust density with each subsequent revolution.

Regarding the decay of dust density with subsequent revolutions, we assume that the dust density falls off inversely with the number of revolutions (N), which is expected if the spreading is mainly due to differences in orbital period of the particles in the dust traillet. Here, we ignore the fact that the peak of the particle density also shifts progressively along the comet orbit in time. In that case, the peak dust density at a given position after 1 revolution is:

$$\text{ZHR}_{\text{max}}^t (1 \text{ rev.}) = \text{ZHR}_{\text{max}}^t \times N \quad (7)$$

Figure 10 shows the density of dust in the center of the traillet after one revolution, calculated from the observed peak ZHR value. This value was corrected to a center-of-traillet value for a Lorentz distribution with adopted $W_t = 0.00032$ AU perpendicular to Earth's orbit centered on the trail centers calculated by McNaught and Asher (1999b), and by taking Equation 7 into account. Unfortunately, only one data point (the return of 1969) is available to constrain the slope of the dashed line in Figure 10. All other observations fall in a rather narrow range of mean anomaly. Any error in the 1969 result will bear heavily on the assumed dependence on mean anomaly and the predictions that follow from it.

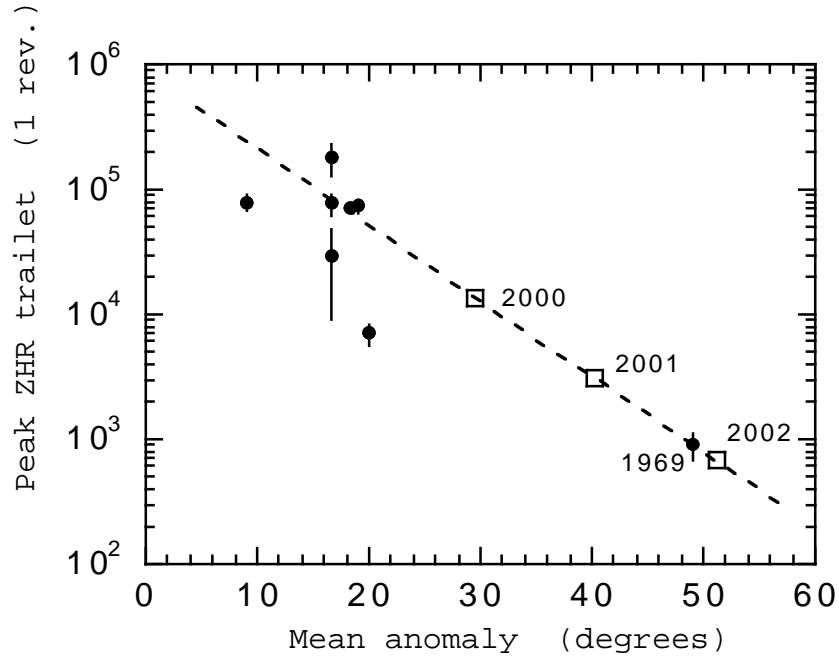


Figure 10. Peak dust density in the traillet after 1 revolution, as derived from the flux profiles of past meteor storms and outbursts. Three lower points all refer to pre 1899 traillets.

From Figure 10, it is possible to predict the peak activity in 2000–2002. The time since perihelion passage for each return is marked on the dashed line with an open square. The predicted peak rate follows from this by corrections according to Equation 7 and Equation 6. We find $ZHR = 70$ in 2000 (1866 traillet), $ZHR = 210$ in 2000 (1932 traillet), $ZHR = 70$ in 2001 (1866) and $ZHR = 40$ in 2002 (1866), whereby the width of the profiles should gradually decrease from $W = 0.0022$ AU (1866) and 0.0018 AU (1932) in 2000 to $W = 0.0011$ AU in 2001 and 0.0007 AU in 2002.

These predictions are somewhat disappointing given the high predicted rates by McNaught and Asher (1999b) of 10–35,000 and 25,000 for the 1866 traillet encounter of 2001 and 2002, respectively. However, one should keep in mind that the observations on which these predictions are based are very limited. Also, the expected rates are higher if we would include the anticipated progressive shift of the peak of the particle density along the comet orbit in time.

4.1. FUTURE OBSERVATIONS

The video record of the 1999 Leonid meteor storm is a treasure trove of information that can be further analyzed. Unlike the hybrid visual-video observation technique, such in-depth analysis is time consuming. Some preliminary results are presented in Gural and Jenniskens (2000).

After full analysis of the 1999 shower, the big unknown will still be the dispersion perpendicular to Earth's path and the exact position of the dust trail center. Only the year 2000 encounter can shed light on this. The predicted distances to the traillet centers are small enough to get significant increased rates and recognize the component from other shower components. Also, the distance to the traillet center is not as small as in 2001 and 2002, when we are on the steep slope of the Lorentz profile. Small natural shifts in the trail center can cause great variations in rates that are can not easily be interpreted in terms of the width of the dust trail perpendicular to the Earth's path. On the other hand, while the year 2000 provides a 2-dimensional picture of what is now only a 1-dimensional view of dust trails, the years 2001 and 2002 will provide a three dimensional perspective by providing important clues to how quickly the dust density falls off away from the comet position.

The method described in this paper promises a detailed picture of the dust density in comet dust traillets by combining theory and observations of future Leonid showers. Observations in future years will test the assumptions that go into the model, such as the cylindrical geometry and the position of the trail. Each future encounter will be a strong test for refining the theoretical multi-traillet model of comet dust trails.

Acknowledgements

We thank ESA's Michael Schmidhuber for assisting in the "flux measurement team" and Morris Jones and Pete Gural who assisted in the visual examination of the FISTA tapes after the flight. The flux measurements in the Leonid MAC 1999 mission were supported by grants from USAF/XOR and the NASA Planetary Astronomy and Suborbital MITM programs. *Editorial handling:* Noah Brosch.

References

- Asher, D.: 1999, *MNRAS* **307**, 919–924.
- Arlt, R. and Brown, P.: 1999, *WGN, Journal of the IMO* **27**, 267–285.
- Arlt, R., Bellot-Rubio, L., Brown, P., and Gijssens, M.: 1999, *WGN, Journal of the IMO* **27**, 286–295.
- Brown, P., Simek, M., and Jones, J.: 1997, *Astron. Astrophys.* **322**, 687–695.
- Gural, P. and Jenniskens, P.: 2000, *Earth, Moon and Planets* **82–83**, 221–248.
- Jenniskens, P.: 1995, *Astron. Astrophys.* **295**, 206–235.
- Jenniskens, P.: 1996, *Meteoritics Planet. Sci.* **31**, 177–184.
- Jenniskens, P.: 1999, *Meteoritics Planet. Sci.* **34**, 959–968.
- Jenniskens, P. and Butow, S.J.: 1999, *Meteoritics Planet. Sci.* **34**, 933–943.
- Jenniskens, P. and Betlem, H.: 2000, *Astrophys. J.* **531**, 1161–1167.
- Jenniskens, P., Butow, S.J., and Fonda, M.: 2000, *Earth, Moon and Planets* **82–83**, 1–26.
- Kondrat'eva, E.D. and Reznikov, E.A.: 1985, *Sol. Syst. Res.* **19**, 96–101.
- Lyytinen, E.: 1999, *Meta Research Bulletin* **8**, 33–40.
- McNaught, R.H. and Asher, D.J.: 1999a, *Meteoritics Planet. Sci.* **34**, 975–978.
- McNaught, R.H., and Asher, D.J.: 1999b, *WGN, Journal of the IMO* **27**, 85–102.